⌘ *Author's Choice*

THE JOURNAL OF BIOLOGICAL CHEMISTRY VOL. 285, NO. 10, pp. 7598–7609, March 5, 2010

Proteoliposomes Harboring Alkaline Phosphatase and Nucleotide Pyrophosphatase as Matrix Vesicle Biomimetics*[S]

Received for publication, October 27, 2009, and in revised form, December 15, 2009 Published, JBC Papers in Press, January 4, 2010, DOI 10.1074/jbc.M109.079830

Ana Maria S. Simão[‡§1], Manisha C. Yadav[§], Sonoko Narisawa[§], Mayte Bolean[‡], Joao Martins Pizauro[¶], Marc F. Hoylaerts[§‖], Pietro Ciancaglini[‡§], and José Luis Millán[§2]

From the [‡]Department of Chemistry, Faculdade de Filosofia, Ciências e Letras de Ribeirão Preto, Universidade de São Paulo, Ribeirão Preto SP 14040-901, Brazil, the [§]Sanford Children's Health Research Center, Burnham Institute for Medical Research, La Jolla, California 92037, the [¶]Department of Technology, Faculdade de Ciências Agrárias e Veterinárias de Jaboticabal, Universidade Estadual Paulista, Jaboticabal SP 14884-900, Brazil, and the [‖]Center for Molecular and Vascular Biology, University of Leuven, B-3000, Leuven, Belgium

We have established a proteoliposome system as an osteoblast-derived matrix vesicle (MV) biomimetic to facilitate the study of the interplay of tissue-nonspecific alkaline phosphatase (TNAP) and NPP1 (nucleotide pyrophosphatase/phosphodiesterase-1) during catalysis of biomineralization substrates. First, we studied the incorporation of TNAP into liposomes of various lipid compositions (*i.e.* in pure dipalmitoyl phosphatidylcholine (DPPC), DPPC/dipalmitoyl phosphatidylserine (9:1 and 8:2), and DPPC/dioctadecyl-dimethylammonium bromide (9:1 and 8:2) mixtures. TNAP reconstitution proved virtually complete in DPPC liposomes. Next, proteoliposomes containing either recombinant TNAP, recombinant NPP1, or both together were reconstituted in DPPC, and the hydrolysis of ATP, ADP, AMP, pyridoxal-5′-phosphate (PLP), *p*-nitrophenyl phosphate, *p*-nitrophenylthymidine 5′-monophosphate, and PP_i by these proteoliposomes was studied at physiological pH. *p*-Nitrophenylthymidine 5′-monophosphate and PLP were exclusively hydrolyzed by NPP1-containing and TNAP-containing proteoliposomes, respectively. In contrast, ATP, ADP, AMP, PLP, *p*-nitrophenyl phosphate, and PP_i were hydrolyzed by TNAP-, NPP1-, and TNAP plus NPP1-containing proteoliposomes. NPP1 plus TNAP additively hydrolyzed ATP, but TNAP appeared more active in AMP formation than NPP1. Hydrolysis of PP_i by TNAP-, and TNAP plus NPP1-containing proteoliposomes occurred with catalytic efficiencies and mild cooperativity, effects comparable with those manifested by murine osteoblast-derived MVs. The reconstitution of TNAP and NPP1 into proteoliposome membranes generates a phospholipid microenvironment that allows the kinetic study of phosphosubstrate catabolism in a manner that recapitulates the native MV microenvironment.

During endochondral bone formation, chondrocytes and osteoblasts mineralize their extracellular matrix by promoting the initial formation of crystalline hydroxyapatite (HA)[3] (1). Experimental evidence has pointed to the presence of HA crystals along collagen fibrils in the ECM and also within the lumen of chondroblast- and osteoblast-derived matrix vesicles (MVs). Two phosphatases have been implicated during MV-mediated calcification (*i.e.* tissue-nonspecific alkaline phosphatase (TNAP; EC 3.1.3.1) and NPP1 (nucleotide pyrophosphatase/phosphodiesterase-1) (EC 3.6.1.9) (2, 3). In skeletal tissue, TNAP is confined to the cell surface of osteoblasts and chondrocytes, including the membranes of their shed MVs (4, 5). In fact, by an unknown mechanism, MVs are markedly enriched in TNAP compared with both whole cells and the plasma membrane (6). It has been proposed that the role of TNAP in the bone matrix is to generate the inorganic phosphate needed for hydroxyapatite crystallization (7–9). However, TNAP has also been hypothesized to hydrolyze the mineralization inhibitor PP_i (10) to facilitate mineral precipitation and growth (11, 12). Electron microscopy revealed that TNAP-deficient MVs, in both humans and mice, contain apatite crystals but that extravesicular crystal propagation is retarded (13–15). This growth retardation could be due to either the lack of a TNAP pyrophosphatase function or the lack of inorganic phosphate generation. Our recent studies have provided compelling proof that the function of TNAP in bone tissue consists of hydrolyzing PP_i to maintain a proper concentration of this mineralization inhibitor to ensure normal but not ectopic bone mineralization (3, 16, 17).

PP_i is generated by the ectonucleotide pyrophosphatase/phosphodiesterase (NPP) family of isozymes. PC-1 (plasma cell membrane glycoprotein-1) (more correctly termed NPP1) is plasma membrane-bound, whereas autotaxin (NPP2) is

* This work was supported, in whole or in part, by National Institutes of Health Grants DE12889, AR47908, and AR53102, by a grant from the Thrasher Research Fund, and by grants from the Fundação de Amparo à Pesquisa do Estado de São Paulo, Coordenação de Aperfeiçoamento de Pessoal de Nível Superior (CAPES), and Conselho Nacional de Desenvolvimento Científico e Tecnológico (CNPq). The Center for Molecular and Vascular Biology is supported by the "Excellentie Financiering KULeuven" (EF/05/013).

⌘ *Author's Choice*—Final version full access.

[S] The on-line version of this article (available at http://www.jbc.org) contains supplemental Fig. 1.

[1] Recipient of studentships from FAPESP.

[2] To whom correspondence should be addressed: Sanford Children's Health Research Center, Burnham Institute for Medical Research, 10901 N. Torrey Pines Rd., La Jolla, CA 92037. Tel.: 858-646-3130; Fax: 858-646-3195; E-mail: millan@burnham.org.

[3] The abbreviations used are: HA, hydroxyapatite; AMPOL, 2-amino-2-methyl-propan-1-ol; DODAB, dioctadecyl-dimethylammonium bromide; DPPC, dipalmitoyl phosphatidylcholine; DPPS, dipalmitoyl phosphatidylserine; GPI, glycosylphosphatidylinositol; MV, matrix vesicle; GPI, glycosylphosphatidylinositol; PLC, phospholipase C; PLP, pyridoxal-5′-phosphate; *p*NPP, *p*-nitrophenyl phosphate; *p*NPPase, *p*-nitrophenylphosphatase; *p*NP-TMP, *p*-nitrophenylthymidine 5′-monophosphate; *p*NP-TMPase, *p*-nitrophenylthymidine 5′-monophosphatase; polidocanol, polyoxyethylene-9-lauryl ether; TNAP, tissue-nonspecific alkaline phosphatase; NPP, nucleotide pyrophosphatase/phosphodiesterase; CHO, Chinese hamster ovary; HPLC, high pressure liquid chromatography.

secreted and B10 (NPP3) is abundant in intracellular spaces (18). All three isozymes are expressed in a wide variety of tissues, including bone and cartilage (19), and they all have the common ability to hydrolyze diesters of phosphoric acid into phosphomonoesters, primarily ATP to AMP and/or ADP to adenosine. Similar to skeletal TNAP expression, NPP1 is highly abundant on the surfaces of osteoblasts and chondrocytes as well as on the membrane of their MVs (20, 21). NPP1 has a role in inhibiting HA precipitation by its PP_i-generating property. This proposed function has been supported by *in vitro* studies where cells transfected with the NPP1 cDNA resulted in elevated levels of PP_i in osteoblast-derived MVs, accompanied by decreased matrix mineralization (20, 22).

As we strive to understand the physiological interplay between TNAP, NPP1, and other important MV-associated enzymes in the initiation of biomineralization, we must keep in mind the microenvironment in which these enzymes function, which can have a profound effect on their biological properties. Recent data (23) suggest that the location of TNAP on the membrane of MVs plays a role in determining substrate selectivity in this microcompartment. Those data suggested that assays of TNAP bound to MVs or to liposome-based systems might be more biologically relevant than assays done with solubilized enzyme preparations, particularly when studying the hydrolysis of organophosphate substrates. The ability of synthetic or natural vesicles (24, 25) to mimic the organizational structure and function of biomembranes makes these structures an advantageous and convenient experimental model to help us advance our understanding of MV-mediated calcification. Dipalmitoylphosphatidylcholine (DPPC) liposomes have already been shown to be capable of sequestering ions and promoting calcium phosphate deposition *in vitro* and thus represent a good first choice for the development of an MV biomimetic system (26). Here we describe the production and characterization of proteoliposomes harboring TNAP alone, NPP1 alone, and TNAP + NPP1 together as MV biomimetics to help us understand the interplay between these enzymes, crucial during early events of skeletal mineralization.

EXPERIMENTAL PROCEDURES

TNAP and NPP1 Expression Constructs—The 2.5-kb human TNAP cDNA was cloned into pCMV-Script vector (Stratagene, La Jolla, CA) to express native form of TNAP. A plasmid containing rat NPP2 N-terminal signal peptide (33 residues) connected to the residues of mouse NPP1 (residues 85–905) was kindly provided by Dr. Bollen (28). To produce a GPI-anchored form of mouse NPP1, 2.4 kb of mouse NPP1 coding sequence corresponding to the peptide 85–905 was PCR-amplified from the chimeric cDNA by *pfx* polymerase (Invitrogen) with 5′-primer (5′-CCG CGG GAA GTA AAA AGT TGC AAA-3) and 3′-primer (5′-GTC TTC TTG GCT GAA GAT TGG CAA-3′). We previously produced an expression construct in pCMV-Script vector to produce human PLAP, which originally contained a signal peptide sequence at the N terminus and a GPI-anchoring sequence near the C terminus. A 4.9-kb DNA fragment covering the signal peptide region-pCMV-Script vector-GPI anchoring site was PCR-amplified from the PLAP-pCMV-Script vector by *pfx* polymerase (Invitrogen) with 5′-primer (5′-CTG GCG CCC CCC GCC GGC AC-3′) and 3′-primer (5′-AAC TGG GAT GAT GCC CAG GGA GAG C-3′). The 2.4-kb mouse NPP1 fragment was inserted into the 4.9-kb vector containing the PLAP signal peptide and GPI anchoring site. The PCR-amplified sequences and framing of the connections were confirmed by direct sequencing.

Expression of TNAP and NPP1—CHO-K1 (Chinese hamster ovary, ATCC number CCL-61) cells were trypsinized, and 1.0×10^7 cells were suspended in 800 μl of HEPES-buffered saline, containing 10 μg of plasmid of human TNAP cDNA in pCMV-Script vector. The cell suspension was placed in an electroporation cuvette (4-mm distance) and electroporated at 400 mV, 250 microfarads using Gene Pulser (Bio-Rad). After incubation on ice for 20 min, the electroporated cell suspension was diluted ~250 times with growth medium (10% fetal calf serum, Dulbecco's modified Eagle's medium) and seeded onto 15-cm dishes. Twenty-four hours later, the medium was replaced by selection medium containing 800 μg/ml G418, and the selection medium was renewed every third day. Two weeks later, G418-resistant cells were harvested for the preparation of membrane samples for TNAP. COS-1 (ATCC number CRL-1650) cells were trypsinized, and 1.0×10^7 cells were suspended in 800 μl of HEPES-buffered saline, containing 10 μg of plasmid of mouse NPP1 with a signal peptide/GPI anchoring site in pCMV-Script. The cell suspension was electroporated at 220 mV, 960 microfarads. After incubation on ice for 20 min, the electroporated cells were seeded onto 15-cm dishes, and cells were harvested 60 h later. This transient expression was more efficient for NPP1 expression than the stable expression system using CHO-K1 cells. Western/Northern blot analysis and enzyme activity assays of these cells revealed that both enzymes were produced in good yields.

Preparation of Membrane Fraction Rich in TNAP and NPP1—Membrane-bound TNAP was obtained from 14-day primary osteoblast cultures or from stably transfected CHO-K1 cells as described (31). Membrane-bound NPP1 was obtained from transfected COS-1 cells as described (31).

Solubilization and Partial Purification of GPI-anchored Enzymes with Polyoxyethylene 9-Lauryl Ether—Membrane-bound enzymes (0.2 mg/ml total protein) were solubilized with 1% polidocanol (w/v) (final concentration) for 2 h, with constant stirring, at 25 °C. After centrifugation at 100,000 × *g* for 1 h at 4 °C, the solubilized enzymes were concentrated as described previously (32). Detergent-free, solubilized enzymes were obtained using 200 mg of Calbiosorb resin and 1 ml of polidocanol-solubilized enzyme (~0.03 mg of protein/ml), as described previously (24). All protein concentrations were estimated in the presence of 2% (w/v) SDS (33). Bovine serum albumin was used as a standard.

Enzymatic Assays—*p*-Nitrophenylphosphate (*p*NPP) and *p*-nitrophenylthymidine 5′-monophosphate (*p*NP-TMP) activities were assayed discontinuously, at 37 °C, in a spectrophotometer by following the liberation of *p*-nitrophenolate ion (absorbance, 1 M, pH 13, equal to 17,600 M^{-1} cm^{-1}), at 410 nm. Standard conditions were 50 mmol/liter Tris-HCl, pH 7.4, containing 2 mmol/liter $MgCl_2$ and 10 mmol/liter *p*NPP or *p*NP-TMP, in a final volume of 0.5 ml. The reaction was initiated by the addition of the enzyme and stopped with 0.5 ml of 1 mol/

liter NaOH at appropriate time intervals (24). For ATP, ADP, AMP, and PP_i hydrolysis, the phosphomonohydrolase activities were assayed discontinuously by measuring the amount of inorganic phosphate liberated, as before (34), adjusting the assay medium to a final volume of 0.5 ml. Standard assay conditions consisted of 50 mmol/liter Tris-HCl buffer, containing 2 mmol/liter $MgCl_2$ and substrate. All determinations were carried out in duplicate, and initial velocities were constant for at least 90 min, provided that less than 5% of substrate was hydrolyzed. Controls without added enzyme were included in each experiment to correct for non-enzymatic hydrolysis of substrate. One enzyme unit (1 unit/mg) is defined as the amount of enzyme hydrolyzing 1.0 nmol of substrate/min at 37 °C/ mg of protein. Maximum velocity (V_{max}), apparent dissociation constant ($K_{0.5}$), and Hill coefficient (n) obtained from substrate hydrolysis were calculated as described (35). The effect of pH on *p*NPPase, ATPase, and pyrophosphatase activities of TNAP reconstituted in DPPC liposomes was measured in 50 mmol/liter buffer over the pH range of 5.0–10.5. Data were reported as the mean of triplicate measurements of three different enzyme preparations. Statistically significant differences were defined as $p \leq 0.05$.

Liposome Preparation—DPPC or mixtures of DPPC/dipalmitoylphosphatidylserine (DPPS) or DPPC/dioctadecyldimethylammonium bromide (DODAB) at molar ratios of 9:1 and 8:2 were prepared dissolving 1 mg/ml lipids in chloroform. After removing chloroform with a nitrogen flow, the lipid film was resuspended in 50 mmol/liter Tris-HCl buffer, pH 7.5, containing 2 mmol/liter $MgCl_2$, and the mixture was incubated at 60 °C for 60 min, during vigorous stirring, using a vortex at 10-min intervals. The mixture was passed through an extrusion system (Liposofast, Sigma) using a polycarbonate membrane of 100 nm, and the suspension of relatively small homogeneous unilamellar vesicles was stored at 4 °C.

Incorporation of GPI-anchored TNAP and NPP1 into Liposomes—Equal volumes of liposomes (100 nmol of P_i/ml) and TNAP (0.02 mg/ml) or NPP1 (0.02 mg/ml) or TNAP (0.01 mg/ml) plus NPP1 (0.01 mg/ml) in 50 mmol/liter Tris-HCl buffer, pH 7.5, containing 2 mmol/liter $MgCl_2$ were mixed and incubated at 25 °C. At predetermined intervals, 100-μl samples were removed and centrifuged at 100,000 × *g* for 60 min. The pellet was then resuspended in the same buffer to the original volume. The activities of TNAP and NPP1 in the supernatant and resuspended pellet were assayed in order to calculate the percentage of protein incorporation. To confirm the incorporation of the proteins, Western blot analysis of the proteoliposomes was performed using anti-human TNAP antibody (R&D, Minneapolis, MI) and anti-human NPP1 antibody (Everest Biotech).

Light Scattering of Liposomes and Proteoliposomes—The size distribution of liposomes and proteoliposomes was analyzed by dynamic light scattering using a Beckman Coulter submicron particle size analyzer (model N5). The sample was filtered and diluted to an adequate polydispersion index.

Enzymatic Release by TNAP and NPP1—Membrane-bound enzymes or reconstituted proteoliposomes were incubated in 50 mmol/liter Tris-HCl buffer, pH 7.4, with specific phosphatidylinositol phospholipase C (0.2 or 1 unit, as indicated, of GPI-specific PLC from *Bacillus thuringiensis* per ml) for 2 h, under constant rotary shaking, at 37 °C. The incubation mixtures were centrifuged at 100,000 × *g* for 1 h at 4 °C, and the supernatants were concentrated as described previously (23).

Denaturating Polyacrylamide Gel Electrophoresis and Blotting—The molecular mass of the enzymes were estimated by SDS-PAGE (7%) with 5% stacking gel, using silver nitrate for protein staining. Protein samples were concentrated using a Microcon 30 concentrator (Amicon). Phosphohydrolytic activity on the gel was detected in 50 mmol/liter Tris-HCl buffer, pH 7.4, containing 2 mmol/liter $MgCl_2$ and 10 mmol/liter pNP-TMP for NPP1 or in 50 mmol/liter Tris-HCl buffer, pH 7.4, containing 2 mmol/liter $MgCl_2$ and 10 mmol/liter *p*NPP for TNAP, at 37 °C, with 50 mmol/liter Tris-HCl buffer, pH 7.5.

Measurement of Nucleotide Hydrolysis by HPLC—Hydrolysis of ATP, ADP, and AMP by proteoliposomes was determined at 37 °C in 50 mmol/liter Tris-HCl buffer, pH 7.4, containing 2 mmol/liter $MgCl_2$ and substrate. Reactions were started by the addition of enzyme, and, at predetermined intervals, samples were removed and immediately quantified. Nucleotides were separated and quantified by HPLC, injecting a 20-μl aliquot of the sample into a C_{18} reversed-phase column (Shimadzu) and eluting it at 1.5 ml/min, with the mobile phase consisting of 50 mmol/liter potassium-phosphate buffer (pH 6.4), 5 mmol/liter tetrabutylammonium hydrogen sulfate, and 18% (v/v) methanol. $A_{260\ nm}$ was continuously monitored, and nucleotide concentrations were determined from the area under the absorbance peaks.

MV Isolation—Osteoblasts were isolated from 1–3-day-old calvaria as before (3) and plated in 10-cm plates, at a density of 0.75×10^6, in α-minimum Eagle's medium-modified medium (Invitrogen), containing 10% fetal bovine serum. The next day, the medium was replaced with differentiation medium (α-minimum Eagle's medium with 10% fetal bovine serum and 50 μg/ml ascorbic acid). The cells were grown for 18 days, with medium changes every third day. The cell monolayer was washed with media without fetal bovine serum and digested in a collagenase digestion mixture containing 0.45% collagenase (Worthington), 0.12 mol/liter NaCl, 0.01 mol/liter KCl, 1000 units/ml penicillin, 1 mg/ml streptomycin, and 0.05 M Tris buffer (pH 7.6 at 37 °C) (or 2.5 mg/ml collagenase in serum-free medium). Collagenase digestion was done at 37 °C for 1.5–2 h, and the digest was centrifuged at 3,500 rpm for 10 min. The supernatant was subjected to a two-step differential ultracentrifugation, first at 19,500 rpm for 10 min and then at 42,000 rpm for 45 min to obtain the MV pellet.

Negative Staining Electronic Microscopy—Proteoliposomes and MV preparations were visualized by electron microscopy via negative staining. A 5-μl suspension of proteoliposomes and/or MVs was placed on carbon-coated copper grids for 1 min to sediment the sample. The excess buffer was removed and exchanged for 2% (w/v) of an aqueous solution of uranyl-acetate for 15 s; the excess of uranyl-acetate was removed, and grids were air-dried for 2–5 min and placed in a Hitachi H600A transmission electron microscope at 75 kV. Images were collected with an L9C cooled CCD, 11.2-megapixel camera (SIA).

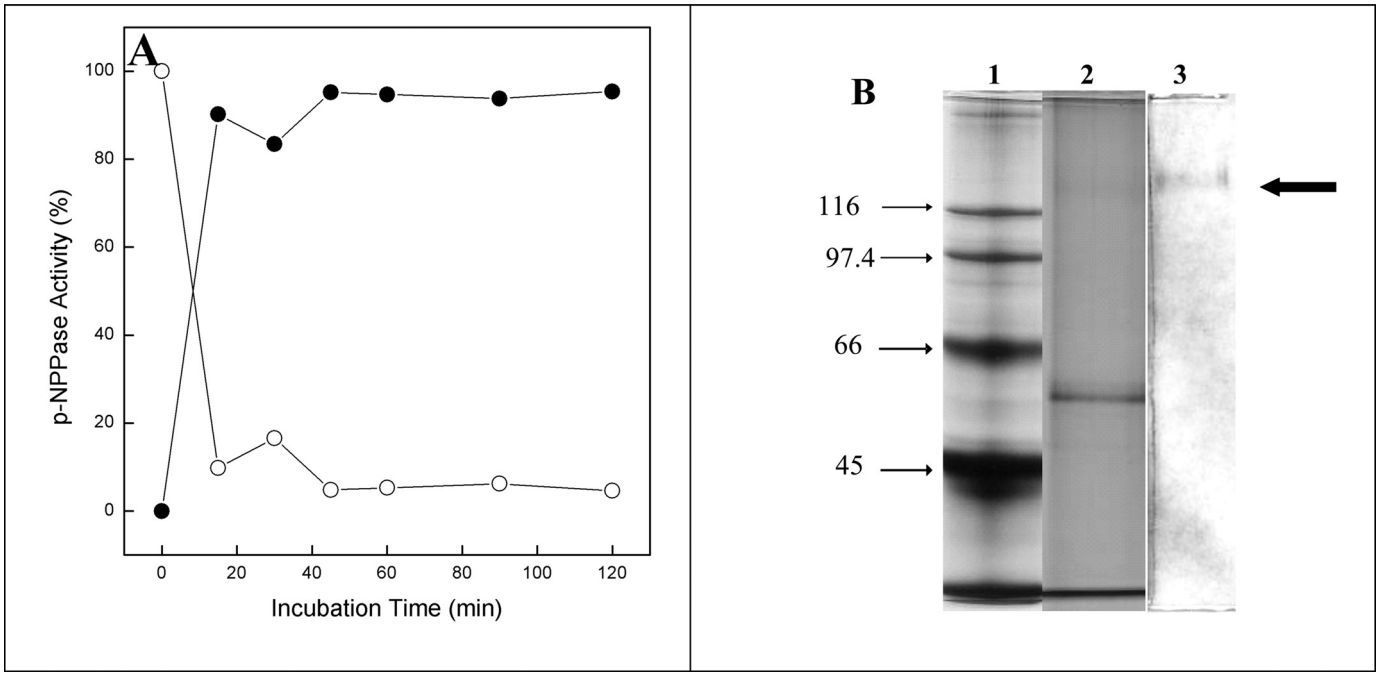

FIGURE 1. **Incorporation of polidocanol-solubilized detergent-free osteoblast-derived TNAP into DPPC liposomes (*A*) and SDS-PAGE of osteoblast-derived TNAP-containing DPPC liposomes (*B*).** *Lane 1*, M_r standards; *lane 2*, TNAP-DPPC proteoliposomes, stained with silver nitrate, of ~60 kDa, corresponding to the monomers of TNAP; *lane 3*, phosphohydrolytic activity of non-denaturated TNAP-DPPC proteoliposomes of ~120 kDa, corresponding to the dimer of TNAP. The *lower bands* in *lanes 1* and *2* represent the leading edge of the gel.

TABLE 1

Reconstitution parameters after osteoblast-derived TNAP incorporation in liposomes with the indicated lipid composition

Composition (mol/mol)	Incubation time	Incorporation	$t_{1/2}$	Liposome size	Proteoliposome size
	min	*%*	*min*	*nm*	*nm*
DPPC	40	90	10	100 ± 25	200 ± 17
DPPC/DPPS (9:1)	240	90	15	85 ± 19	200 ± 11
DPPC/DPPS (8:2)	300	75	240	100 ± 17	270 ± 22
DPPC/DODAB (9:1)	300	50	240	140 ± 23	>1,000
DPPC/DODAB (8/2)	40	90	3.5	170 ± 28	>1,000

RESULTS

Reconstitution of Proteoliposomes Containing TNAP—Detergent removal from the polidocanol-solubilized TNAP by the hydrophobic resin Calbiosorb was deemed to be complete, because methylene proton peaks of ether and lauryl groups of polidocanol were undectectable by NMR in the treated, solubilized enzyme (not shown). This detergent-free osteoblast-derived TNAP quantitatively anchored in DPPC liposomes (Fig. 1*A*) in a time-dependent manner with 90% incorporation in less than 20 min. Empty DPPC liposomes had an average diameter of about 100 nm by dynamic light scattering (Table 1), whereas TNAP proteoliposomes presented diameters of about 200 nm. Electron microscopy of empty DPPC liposomes and TNAP proteoliposomes showed that enzyme reconstitution did not affect the DPPC liposome morphology (not shown). Treatment of TNAP proteoliposomes with GPI-specific PLC released ~60% of the TNAP enzymatic activity into the medium by treatment with 0.2 units of GPI-specific PLC from *Bacillus thuringiensis* per ml for 2 h. Approximately 98% release could be obtained by increasing the amount of GPI-specific PLC to 1.0 units/ml.

The incorporation of detergent-free osteoblast-derived TNAP into liposomes composed of DPPC/DPPS (9:1), DPPC/DPPS (8:2), DPPC/DODAB (9:1), or DPPC/DODAB (8:2), respectively, is shown in the supplemental Fig. 1. In the case of DPPC/DPPS (9:1), DPPC/DPPS (8:2), and DPPC/DODAB (8:2) liposomes, nearly complete TNAP incorporation was achieved after 4 h, 5 h, and 40 min, respectively. TNAP reconstituted into DPPS liposomes to the same degree as in DPPC liposomes but considerably more slowly. In contrast, the TNAP uptake in DPPC/DODAB (8:2) liposomes was very similar to that for DPPC liposomes, with 90% of the enzyme incorporated after 40 min. Incorporation in DPPC/DODAB (9:1) liposomes was inefficient; only about 50% of the *p*NPPase enzyme activity was taken up, even after 5 h. Dynamic light scattering revealed sizes for the empty mixed DPPC/DPPS (9:1), DPPC/DPPS (8:2), DPPC/DODAB (9:1), and DPPC/DODAB (8:2) liposomes of 85, 100, 140, and 170 nm, respectively (Table 1). The average diameters of the corresponding TNAP proteoliposomes were 200 and 270 nm when reconstituted in DPPC/DPPS (9:1) or DPPC/DPPS (8:2) liposomes, respectively (Table 1). Proteoliposomes, reconstituted from DPPC/DODAB (9:1) and DPPC/DODAB (8:2) liposomes, appeared to have a size larger than 1,000 nm. SDS-PAGE of the DPPC proteoliposomes revealed, by silver staining, only a single protein band (Fig. 1*B*, *lane 2*) of about

TABLE 2

Kinetic parameters for the hydrolysis of the indicated substrates by TNAP present in the membrane fraction prepared from osteoblasts or reconstituted in liposomes with the indicated lipid composition

Data are reported as the mean ± S.D. of triplicate measurements.

Substrates	Kinetic parameters	Membrane fraction	Proteoliposomes				
			DPPC	DPPC/DPPS (9:1)	DPPC/DPPS (8:2)	DPPC/DODAB (9:1)	DPPC/DODAB (8:2)
*p*NPP[a]	V_m (units/mg)[b]	1,202 ± 36	4,571 ± 111	3,443 ± 107	3,986 ± 99	5,259 ± 87	5,065 ± 127
	$K_{0.5}$ (mM)	0.16 ± 0.01	0.17 ± 0.02	0.20 ± 0.04	0.27 ± 0.02	0.14 ± 0.03	0.19 ± 0.04
	n	0.90 ± 0.05	1.01 ± 0.05	1.00 ± 0.05	1.02 ± 0.05	0.94 ± 0.06	0.91 ± 0.05
	$k_{cat}/K_{0.5}$ (M^{-1} s^{-1})	1.5×10^4	5.4×10^4	3.4×10^4	3.0×10^4	7.5×10^4	5.3×10^4
ATP[a]	V_m (units/mg)	241 ± 9	1,237 ± 26	512 ± 13	563 ± 19	960 ± 17	818 ± 15
	$K_{0.5}$ (mM)	1.5 ± 0.03	1.4 ± 0.04	1.3 ± 0.01	1.5 ± 0.03	0.23 ± 0.01	1.1 ± 0.02
	n	1.00 ± 0.05	1.20 ± 0.05	4.21 ± 0.05	1.70 ± 0.09	1.05 ± 0.06	0.93 ± 0.09
	$k_{cat}/K_{0.5}$ (M^{-1} s^{-1})	3.2×10^2	1.8×10^3	7.9×10^2	7.5×10^2	8.3×10^3	1.5×10^3
PP_i[a]	V_m (units/mg)	366 ± 17	691 ± 21	654 ± 12	738 ± 18	896 ± 19	1,340 ± 31
	$K_{0.5}$ (mM)	2.7 ± 0.07	2.0 ± 0.05	2.1 ± 0.06	2.1 ± 0.04	1.6 ± 0.02	2.0 ± 0.03
	n	1.30 ± 0.09	4.91 ± 0.16	4.60 ± 0.15	6.70 ± 0.17	5.83 ± 0.16	5.00 ± 0.15
	$k_{cat}/K_{0.5}$ (M^{-1} s^{-1})	2.7×10^2	6.9×10^2	6.2×10^2	7.0×10^2	1.1×10^3	1.3×10^3

[a] Units/mg are expressed as nmol of phosphate released/min/mg of liposome-associated protein.

[b] Kinetic analysis was performed at the optimal pH for each substrate (pH 9.0 for PP_i, pH 9.5 for ATP, and pH 10 for *p*NPP) in AMPOL buffer, as described under "Experimental Procedures."

60 kDa, corresponding to the TNAP monomers. When proteoliposomes were submitted to non-denaturating electrophoresis and stained for phosphomonohydrolase activity (Fig. 1*B*, *lane 3*), only a single distinct band of about 120 kDa, corresponding to the TNAP dimer, was observed.

Functional Enzymatic Properties of TNAP Proteoliposomes—The optimum pH for the hydrolysis of *p*NPP, PP_i, and ATP by osteoblast-derived membrane-bound TNAP and liposome-reconstituted osteoblast-derived TNAP was 10, 9, and 9.5, respectively (not shown). To investigate the impact of the liposome phospholipid composition on the activity of liposome-reconstituted TNAP, the kinetic parameters for the hydrolysis of known major TNAP substrates (ATP, PP_i, and *p*NPP) were determined. Hence, Table 2 summarizes the results for the catalysis by osteoblast-derived TNAP, analyzed as native membrane-bound enzyme and as reconstituted enzyme in the various proteoliposomes. Fig. 2 illustrates how the activity of membrane-bound or liposome-reconstituted osteoblast-derived TNAP depends on substrate concentration. When *p*NPP was used as substrate (Fig. 2*A*), TNAP showed classical Michaelis-Menten behavior, cooperative effects were not observed, and $K_{0.5}$ values were similar between the different proteoliposomes tested (Table 2). Substrate inhibition was absent, even at 10 mmol/liter *p*NPP, and the catalytic efficiency ($k_{cat}/K_{0.5}$) was comparable between the different proteoliposomes (Table 2). Because V_{max} and $k_{cat}/K_{0.5}$ were expressed as normalized values (units/mg total protein), lower activities were measured for the membrane fraction than for the proteoliposomes (Table 2).

During hydrolysis of ATP by liposome-reconstituted TNAP (Fig. 2*B*), different saturation curves were obtained for the different proteoliposomes, with variable V_{max} and up to a 6-fold lower $K_{0.5}$ in DPPC/DODAB proteoliposomes than for cell membrane-bound TNAP (Table 2) or DPPC/DPPS (8:2) proteoliposomes (Fig. 2*B*). Correspondingly, catalytic efficiencies were up to 10-fold different between DPPC/DODAB (9:1) and DPPC/DPPS (8:2) proteoliposomes (Table 2). Inhibition of ATPase activity was observed for [ATP] of >8 mmol/liter, in the case of the DPPC proteoliposomes, >5 mmol/liter for the DODAB proteoliposomes, and >7 mmol/liter for DPPS proteoliposomes. Fig. 2*B* illustrates weak positive cooperativity during ATP hydrolysis by DPPC-bound TNAP, a property found to be more pronounced with TNAP reconstituted in DPPC/DPPS (9:1) liposomes (Table 2). Hence, the specific phospholipid microenvironment was a co-determinant of the TNAP activity during hydrolysis of ATP.

Hydrolysis of PP_i by reconstituted TNAP (Fig. 2*C*) was positively cooperative in all proteoliposomes, and $K_{0.5}$ values were similar (Table 2). The maximal rates of substrate conversion (V_{max}) differed more than 3-fold between proteoliposomes. Inhibition of the enzyme pyrophosphatase activity occurred for [PP_i] of >5 mmol/liter with DPPC-reconstituted TNAP and >4 mmol/liter with DODAB- and DPPS-reconstituted TNAP (*i.e.* at concentrations just above those saturating TNAP (at V_{max})). The direct comparison of the catalytic efficiency for membrane-bound TNAP showed that V_{max} for hydrolysis of *p*NPP was 4-fold higher than for ATP and PP_i (Fig. 2*D*). These experiments illustrate that the phospholipid microenvironment influenced enzyme catalysis by TNAP differentially for the various substrates.

Reconstitution and Characterization of Proteoliposomes Containing Recombinant TNAP and Recombinant NPP1—Membrane fractions from CHO-K1 cells transfected with the human TNAP cDNA expression vector revealed around 46.8 units/mg *p*NPPase activity, whereas NPP1-transfected COS-1 cells expressed NPP1 with activities around 18.5 units/mg *p*NP-TMPase activity (not shown). When TNAP was solubilized with polidocanol at 1% (w/v), 45% of the proteins were solubilized, with a *p*NPPase activity of 46.5 units/mg. After detergent removal, 50% of the total protein was recovered, resulting in a *p*NPPase activity of about 55.7 units/mg. Solubilization of NPP1 resulted in 44% solubilized protein, with a *p*NP-TMPase activity of 63.5 units/mg (Table 3), and about 44% of total protein was recovered, resulting in a *p*NP-TMPase activity of about 42.6 units/mg (Table 3).

Both polidocanol-solubilized detergent-free enzymes anchored to DPPC liposomes after 2 h of incubation. For TNAP, about 57% of the protein was reconstituted into the liposomes, resulting in a *p*NPPase activity of about 40.5 units/mg (94% of the activity). For NPP1, about 54% of the protein was incorporated, resulting in a *p*NP-TMPase activity of about 45.3 units/mg (80% of the activity) (Table 3). The size of the human TNAP and NPP1 proteoliposomes, determined

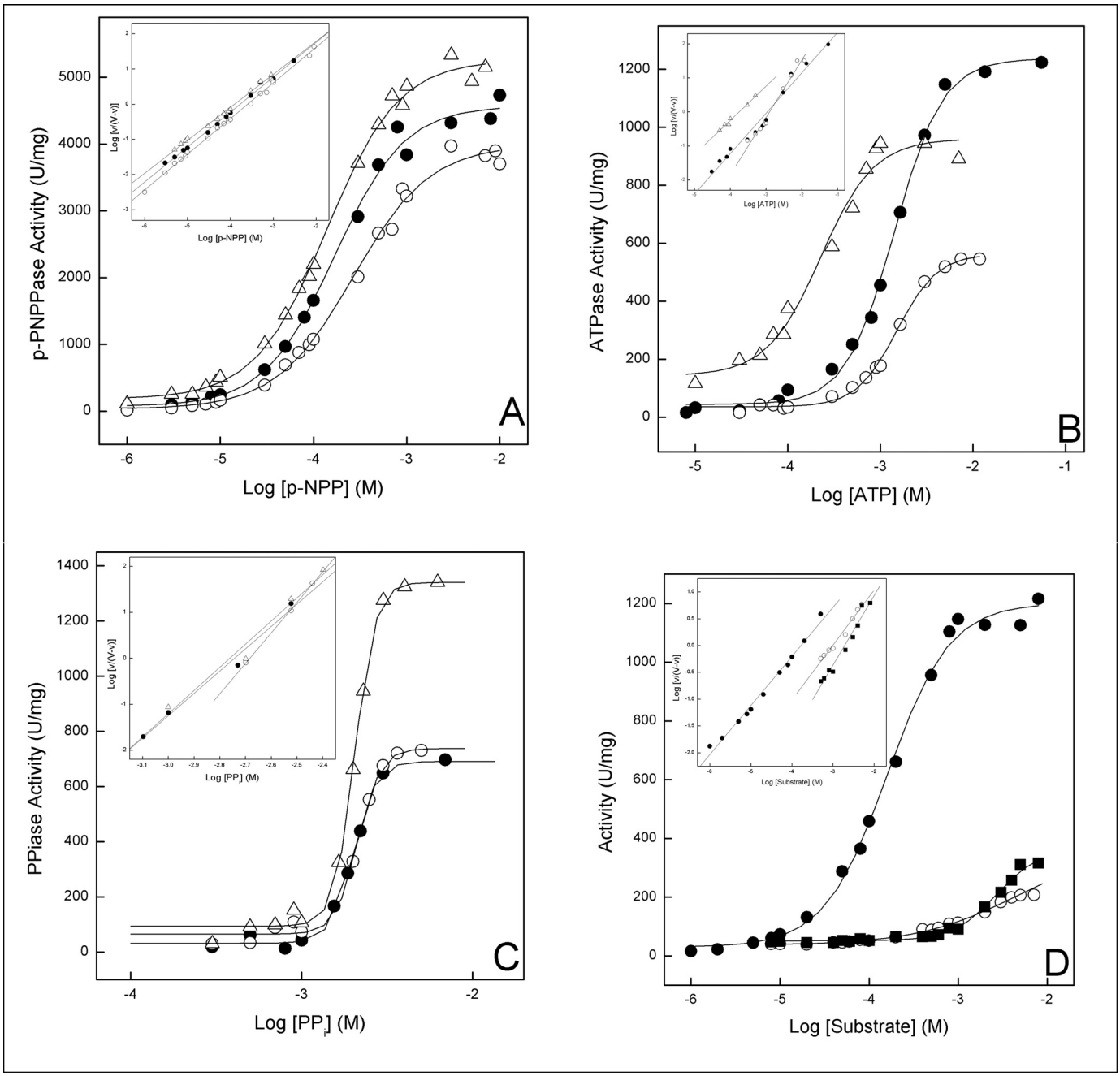

FIGURE 2. **Kinetic activity of liposome-associated osteoblast-derived TNAP.** Shown is hydrolysis of *p*NPP (*A*), ATP (*B*), and PP_i (*C*) for TNAP reconstituted in DPPC (●), DPPC/DPPS (8:2) (○), and DPPC/DODAB (9:1) (△) liposomes (*A*); DPPC (●), DPPC/DPPS (8:2) (○), and DPPC/DODAB (9:1) (△) liposomes (*B*); and DPPC (●), DPPC/DPPS (8:2) (○), and DPPC/DODAB (8:2) (△) liposomes (*C*). *D*, hydrolysis of *p*NPP (●), ATP (○), and PP_i (■). Assays were determined at 37 °C in 50 mmol/liter AMPOL, containing 2 mmol/liter $MgCl_2$, pH 10.0 (*p*NPP), pH 9.5 (ATP), and pH 9.0 (PP_i). *Inset*, Hill plot of the interaction of the substrate with the enzyme.

by dynamic light scattering, was 300 and 400 nm, respectively. The simultaneous reconstitution of detergent-free TNAP and detergent-free NPP1 in DPPC liposomes, after 2 h of incubation, resulted in about 79% TNAP and 82% NPP1 incorporation. The resulting TNAP + NPP1 proteoliposomes had a *p*NPPase activity of 25.8 units/mg and a *p*NP-TMPase activity of 26.4 units/mg (Table 3). The average diameter of these proteoliposomes systems was 380 nm.

Western blotting analysis on the liposome samples showed that CHO-K1 cell-derived TNAP and COS-1 cell-derived NPP1 enzymes were incorporated into the liposomes, and the amount of TNAP or NPP1 protein in the TNAP + NPP1 proteoliposome sample was approximately half of the TNAP and NPP1 samples, respectively (Fig. 3).

The kinetic characteristics of CHO-K1 cell-derived human TNAP-, COS-1 cell-derived mouse NPP1-, and TNAP plus NPP1 proteoliposomes were then studied (Table 4) in comparison with murine primary osteoblast-derived MVs. The TNAP proteoliposomes showed broad substrate specificity at pH 7.4 and hydrolyzed *p*NPP, ATP, ADP, AMP, pyridoxal-5′-phosphate (PLP) (exclusively hydrolyzed by TNAP), and PP_i. NPP1 proteoliposomes also presented broad substrate specificity but

TABLE 3

Summary of polidocanol solubilization, detergent removal, and different reconstitution steps in DPPC liposomes for human TNAP and NPP1 isolated from transfected CHO-K1 and COS-1 culture cells, respectively

Enzymes	CHO-K1 or COS-1 cells							Proteoliposomes			
	Membrane fraction	Total protein solubilized[a]			Detergent removal			Incorporation			Protein yield
	mg/ml	*mg/ml (%)*	*units/ml*	*units/mg*[b]	*mg/ml (%)*	*units/ml*	*units/mg*	*mg/ml (%)*	*units/ml (%)*	*units/mg*[b]	*%*
NPP1[c]	1.44	0.0961 (44)	6.1	63.5	0.042 (44)	1.78	42.6	0.055 (54.5)	2.49 (80.6)	45.3	57.2
TNAP[d]	1.36	0.0987 (45)	4.6	46.5	0.049 (50)	2.75	55.7	0.055 (56.7)	2.23 (94)	40.5	55.7
NPP1 + TNAP								0.055 (48.3)	1.45 (82)[c] 1.42 (79.5)[d]	26.4[c] 25.8[d]	56.5

[a] Initial concentration was adjusted to 0.2 mg/ml of total protein.
[b] Units/mg correspond to nmol of phosphate released/min/mg of total protein.
[c] Activity monitored by hydrolysis of p-nitrophenyl-5'-monophosphate (10 mmol/L), pH 7.4 (1 mmol/L EDTA fully inhibits activity).
[d] Activity monitored by hydrolysis of *p*-nitrophenylphosphate (10 mmol/liter), pH 7.4 (1 mmol/liter $ZnCl_2$ fully inhibits activity).

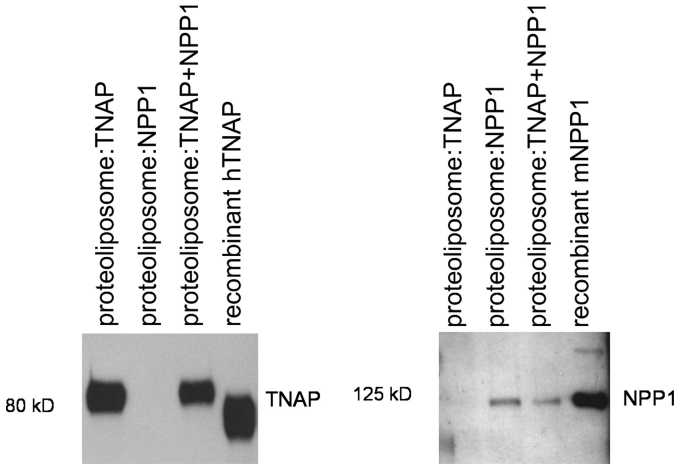

FIGURE 3. **Western blot analysis of proteoliposomes containing recombinant TNAP derived from CHO-K1 cells, recombinant NPP1 derived from COS-1 cells, and TNAP plus NPP1.** Each lane was loaded with titered amounts of proteoliposomes. Positive controls are 15 ng of recombinant human TNAP and 50 ng of recombinant mouse NPP1.

with lower velocity rates for all substrates. The highest rate (V_{max}) of hydrolysis was found for *p*NPP and *p*NP-TMP (exclusively hydrolyzed by NPP1) for TNAP and NPP1 proteoliposomes, respectively. At pH 7.4, positive and negative cooperative effects were observed, depending on the substrates used, and the $K_{0.5}$ values were also quite different, varying from 0.016 to 0.71 mmol/liter. The hydrolysis rates of the substrates were higher for liposomes containing TNAP when compared with MVs but lower for NPP1 proteoliposomes, pointing to a major role of TNAP in the hydrolysis of these substrates. The catalytic efficiencies were also lower for NPP1 proteoliposomes compared with TNAP proteoliposomes for all substrates, except for ATP, indicating a significant participation of NPP1 in the hydrolysis of ATP, despite its low velocity rate. Hence, the comparable reactivity pattern of TNAP, NPP1, and TNAP plus NPP1 proteoliposomes (Table 4), for the hydrolysis of the endogenous substrates ATP, ADP, AMP, and PP_i suggested a predominant activity of TNAP in mixed vesicles when compared with NPP1. In agreement with enzyme amounts around 50% in the mixed vesicles, PLP and pNP-TMP hydrolysis were reduced to 50% in the TNAP plus NPP1 proteoliposomes.

To investigate in more detail the nucleotide hydrolysis by the different liposome systems, we monitored the formation of reaction intermediates as a function of time during hydrolysis of ATP and ADP, separating and quantifying the products by HPLC. The amounts of hydrolyzed ATP or ADP and the amounts of ADP and/or AMP produced for the different liposome systems are shown for the hydrolysis of ATP (Fig. 4) and ADP (Fig. 5). HPLC analysis demonstrated that hydrolysis of ATP resulted in ADP and AMP formation by the various proteoliposomes with slightly different efficiencies only, as predicted by Table 4 (Fig. 4). Nonetheless, the time-dependent catalysis of ATP is more pronounced in CHO-K1 cell-derived TNAP proteoliposomes than in the liposomes containing COS-1 cell-derived NPP1, confirming the major role of TNAP in the hydrolysis of this substrate. In accordance with the predominant role of TNAP in the TNAP-containing proteoliposomes, the concentration of the reaction intermediate ADP was higher during processing by TNAP and TNAP plus NPP1 proteoliposomes, and less ADP formation was observed for the NPP1 proteoliposomes (Fig. 4*B*). Likewise, the subsequent degradation product, AMP, accumulated to a similar degree upon incubations with TNAP and TNAP plus NPP1 proteoliposomes (Fig. 4*C*). The relatively larger AMP accumulation by these proteoliposomes, compared with the low AMP accumulation during incubations with NPP1 proteoliposomes, reflects the higher activity of TNAP during ADP formation and its further breakdown to AMP compared with NPP1, generating AMP and PP_i directly, in addition to behaving as a phosphatase (Table 4), as schematically represented in Fig. 6. AMP only accumulated to low levels because it was hydrolyzed itself with high catalytic efficiency to adenosine and phosphate (Table 4).

When ADP was used as a substrate, the highest rate of catalysis was observed (Fig. 5, *ADP*) again for TNAP proteoliposomes (~25% of the initial amount), whereas the rate was comparatively lower for NPP1 proteoliposomes. However, catalysis of ADP by NPP1 proteoliposomes (Table 4 and Fig. 5) confirmed that this enzyme behaves as a phosphatase.

DISCUSSION

Proteoliposomes can be obtained by different preparation techniques, such as mechanical dispersion, sonication, extrusion, solvent dispersion, co-solubilization with detergents, and reverse phase evaporation as well as direct insertion after removal of detergent (36, 37). DPPS and DPPC are two of the main lipids found in the MV membranes, and many studies have revealed that they play a crucial role in the biomineralization process, regulating both calcium entry into the MVs and formation of HA crystals (38–41). Our long term goal is to reconstitute proteoliposomes of increasing complexity that will recapitulate the key events leading to initiation of MV-mediated calcification *in vitro*. Thus, the use of DPPS and DPPC for the

TABLE 4

Kinetic parameters for the hydrolysis of the indicated substrates by DPPC proteoliposomes containing recombinant CHO-K1 cell-derived TNAP, recombinant COS-1 cell-derived NPP1, or TNAP plus NPP1 in comparison with wild type MVs

Substrates	Kinetic parameters	Liposomes			MVs
		TNAP	NPP1	TNAP + NPP1	
ATP[a]	V_m (units/mg)[b]	16.5 ± 1.6	3.30 ± 0.1	15.3 ± 2.1	16.3 ± 0.9
	$K_{0.5}$ (mM)	0.12 ± 0.02	0.016 ± 0.001	0.16 ± 0.03	0.085 ± 0.01
	n	2.1 ± 0.07	3.11 ± 0.3	1.2 ± 0.03	0.7 ± 0.04
	$k_{cat}/K_{0.5}$ ($M^{-1}.s^{-1}$)	382	448		
ADP[a]	V_{max} (units/mg)	22.3 ± 1.9	4.88 ± 0.2	14.0 ± 1.3	8.7 ± 0.6
	$K_{0.5}$ (mM)	0.28 ± 0.05	0.072 ± 0.002	0.15 ± 0.01	0.080 ± 0.03
	n	1.0 ± 0.02	1.2 ± 0.1	2.6 ± 0.02	0.8 ± 0.05
	$k_{cat}/K_{0.5}$ (M^{-1} s^{-1})	207	147		
PP_i[a]	V_m (units/mg)	28.4 ± 0.7	3.66 ± 0.2	14.0 ± 0.9	6.6 ± 0.5
	$K_{0.5}$ (mM)	0.71 ± 0.01	0.070 ± 0.002	0.19 ± 0.02	0.16 ± 0.02
	n	0.90 ± 0.05	0.72 ± 0.05	1.3 ± 0.08	1.0 ± 0.06
	$k_{cat}/K_{0.5}$ (M^{-1} s^{-1})	386	113		
AMP[a]	V_{max} (units/mg)	23.4 ± 1.3	4.73 ± 0.3	16.6 ± 1.7	4.3 ± 0.4
	$K_{0.5}$ (mM)	0.71 ± 0.04	0.20 ± 0.02	0.50 ± 0.01	0.060 ± 0.02
	n	1.4 ± 0.03	0.77 ± 0.03	1.0 ± 0.02	1.2 ± 0.03
	$k_{cat}/K_{0.5}$ (M^{-1} s^{-1})	6077	51		
PLP[a]	V_{max} (units/mg)	16.2 ± 1.3	NH[c]	8.25 ± 0.4	5.4 ± 0.3
	$K_{0.5}$ (mM)	0.48 ± 0.04		0.14 ± 0.05	0.13 ± 0.02
	n	1.4 ± 0.07		2.2 ± 0.3	0.32 ± 0.03
	$k_{cat}/K_{0.5}$ (M^{-1} s^{-1})	67.5			
*p*NPP[a]	V_{max} (units/mg)	32.5 ± 2.3	6.2 ± 0.2	19.0 ± 2.1	8.6 ± 0.4
	$K_{0.5}$ (mM)	0.035 ± 0.001	0.18 ± 0.05	0.020 ± 0.002	1.4 ± 0.01
	n	1.4 ± 0.07	0.57 ± 0.03	1.6 ± 0.06	0.54 ± 0.02
	$k_{cat}/K_{0.5}$ (M^{-1} s^{-1})	1,857	74.6		
*p*NP-TMP[a]	V_{max} (units/mg)	NH	33.9 ± 1.7	18.7 ± 0.4	5.0 ± 0.1
	$K_{0.5}$ (mM)		0.20 ± 0.01	0.051 ± 0.002	0.58 ± 0.05
	n		0.62 ± 0.05	0.60 ± 0.03	0.81 ± 0.05
	$k_{cat}/K_{0.5}$ (M^{-1} s^{-1})		367		

[a] Kinetic analysis was performed in 50 mmol/liter Tris-HCl buffer, pH 7.4, containing 2 mmol/liter $MgCl_2$ as described under "Experimental Procedures."
[b] Units/mg correspond to nmol of phosphate released/min/mg of liposome-associated protein.
[c] NH, not hydrolyzed.

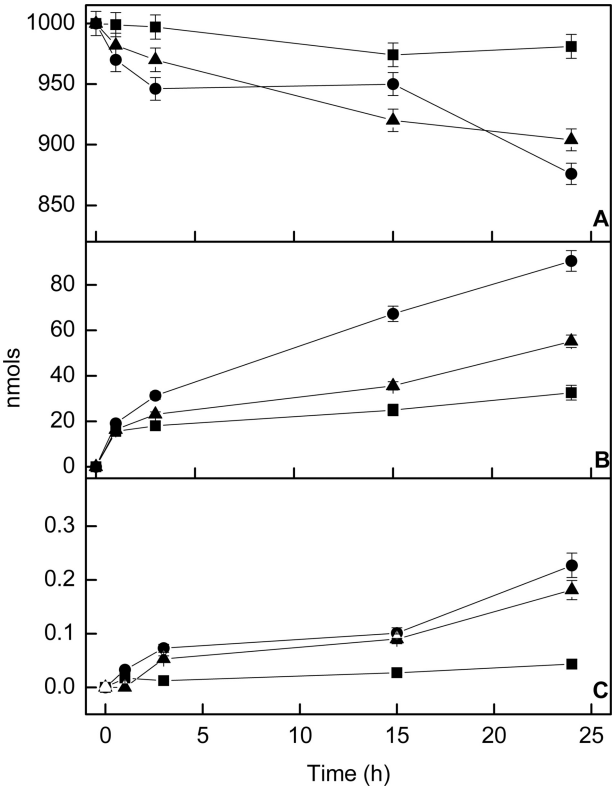

FIGURE 4. **Progression with time of the disappearance of 1,000 nmol of ATP (2 mmol/liter) (*A*) and formation of ADP (*B*) and AMP (*C*), during hydrolysis of ATP by recombinant CHO-K1 cell-derived TNAP-DPPC proteoliposomes (3. 5 μg of total protein) (●), recombinant COS-1 cell-derived NPP1-DPPC proteoliposomes (4.1 μg of total protein) (■), and TNAP + NPP1 proteoliposomes (4.8 μg of total protein) (▲).** The nucleotide concentrations were monitored by HPLC analysis.

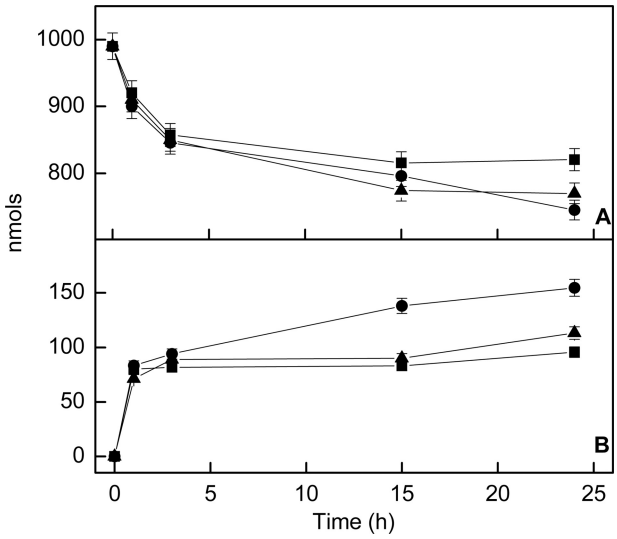

FIGURE 5. **Progression with time of the disappearance of 1,000 nmol of ADP (2 mmol/liter) (*A*) and formation of AMP (*B*) during hydrolysis of ADP by recombinant CHO-K1 cell-derived TNAP-DPPC proteoliposomes (3.5 μg of total protein) (●), recombinant COS-1 cell-derived NPP1-DPPC proteoliposomes (4.1 μg of total protein) (■), and TNAP plus NPP1 proteoliposomes (4.8 μg of total protein) (▲).** The nucleotide concentrations were monitored by HPLC analysis.

reconstitution of proteoliposomes is highly relevant. DODAB was one of the first cationic amphiphiles synthesized (42), with two long hydrocarbon saturated chains. We used it here to evaluate its effects on the physical-chemical and catalytic properties with respect to enzyme integration and catalysis (43, 44).

We found that about 90% of polidocanol-solubilized, detergent-free, TNAP activity was incorporated into DPPC lipo-

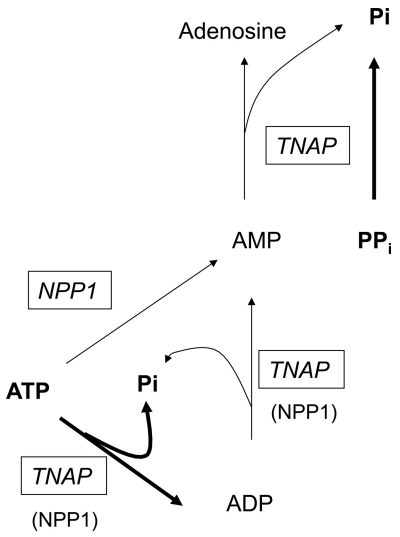

FIGURE 6. **Representation of all the possible simultaneous enzymatic reactions during catalysis of ATP by TNAP and NPP1.** Indicated in *boldface type* are those pathways that are rate-determining in proteoliposomes, simultaneously harboring TNAP and NPP1.

somes via direct insertion. Similar results were observed for the incorporation to DPPC liposomes of the enzyme obtained from rat osseous plate, where 75% of incorporation was obtained with 1 h of incubation (24). The sizes of mixed liposomes constituted by DPPC/DPPS (9:1), DPPC/DPPS (8:2), DPPC/DODAB (9:1), and DPPC/DODAB (8:2), determined by dynamic light scattering, were similar to the expected sizes for vesicles obtained via sonication (36, 37, 45), but the lipid microenvironment modulated the integration of TNAP. TNAP proteoliposomes had diameters around 200 nm. The size of natural osteoblast- and chondrocyte-derived MVs varies from 20 to 300 nm in diameter, and it is not known if a single cell produces multiple subclasses of MVs or only one class at a time (23, 46, 47), so the size of TNAP proteoliposomes reconstituted from DPPC is comparable with the median size of natural MVs (23, 46) and can adequately serve as a vesicular mimetic system.

The lipid charge plays a crucial role in the interaction of proteins with lipids (48–50) and, consequently, with biological membranes. Alkaline phosphatase from bovine intestine interacts in different ways with monolayers constituted by DPPC or DPPS, when inserted into the lipid film, with different effects on the organization of these microenvironments, as a function of the lipid composition (50). Our data are in agreement with these findings. Moreover, the lipid membrane plays an important role as a nucleation agent in the biomineralization process (51, 52) as a protective and/or activation agent (53, 54). Our data indicate that the TNAP-lipid interactions, by modulating the enzyme's catalytic properties, have a functional role in the biomineralization process. Indeed, ATP hydrolysis in DPPC and DPPC/DODAB (9:1) proteoliposomes was quite different. Whereas the $K_{0.5}$ was similar in DPPC proteoliposomes, membrane-bound enzyme from rat osseous plate (55), and membrane-bound enzyme from osteoblasts (31), the $K_{0.5}$ was considerably lower in DPPC/DODAB (9:1) proteoliposomes, and catalysis was non-cooperative. The insertion of negative charges in DPPC/DPPS liposomes induced cooperativity for the hydrolysis of ATP by TNAP.

For PP_i hydrolysis, the $K_{0.5}$ values were similar to that obtained for the membrane-bound enzyme (31), but positive cooperativity was found in all reconstituted liposomes. Different activities have been reported for alkaline phosphatase from rat osseous plate (56, 57). The presently measured enzymatic efficiencies for the hydrolysis of PP_i were up to 200-fold higher in proteoliposomes lacking DODAB. The optimum pH of *p*NPP hydrolysis by TNAP in DPPC liposomes was the same as for membrane-bound enzyme (31) but slightly higher than that for the membrane-bound enzyme from rat bone matrix-induced cartilage (58). For PP_i, the optimum pH of hydrolysis was slightly higher than that for purified membrane-bound enzyme from rat osseous plate (56). The apparent optimum pH for ATP hydrolysis was similar to that for the polidocanol-solubilized enzyme from rat osseous plate (59).

Furthermore, membrane features, such as curvature and lipid composition, can affect enzymatic activity in different ways, depending on the substrate used (24, 60). Sesana *et al.* (60), using proteoliposomes harboring human placental alkaline phosphatase and laser light scattering, demonstrated a strong inverse correlation between activity and liposome diameter. The activity-membrane curvature relationship was further confirmed by comparing the activity of proteoliposomes having different sizes but identical lipid compositions (60). Depending on the protein and phospholipid composition, at physiological pH, we found evidence for the existence both of positive and negative cooperative regulation, providing further evidence that cooperativity was not an intrinsic enzymatic property of TNAP (and/or NPP1) but resulted from secondary interactions with the liposome phospholipids. Indeed, the introduction of structural asymmetry in TNAP dimers results in functional asymmetry and structural allosterism, potentially leading to cooperative interplay between each monomer (61).

The modulation of enzyme activity by the lipid microenvironment seems to be common between enzymes that have a GPI anchor. Lehto and Sharom (62) reported a reduction in the catalytic efficiency of the enzyme 5′-nucleotidase upon insertion of the protein into liposomes with different lipid composition, and the activity could be restored upon enzyme release from the membranes after treatment of the proteoliposomes with GPI-specific PLC. They reported that the degree of activity reduction was dependent on the lipid bilayer where the GPI anchor was inserted, suggesting that different lipids affect the activity of the enzyme in different ways, maybe through alteration in protein conformation transmitted from the membrane to the protein solely through the GPI anchor (63). We have previously documented that although the enzymatic efficiency (k_{cat}/K_m) remained comparable between polidocanol-solubilized and membrane-bound TNAP for all substrates used, the value of k_{cat}/K_m for the GPI-specific PLC-solubilized enzyme increased ~108-, 56-, and 556-fold for *p*NPP, ATP, and PP_i, respectively, compared with the membrane-bound enzyme (23). Changes in the membrane fluidity can also modulate the catalytic properties of anchored proteins through the proximity between the protein and the membrane surface, independently of any conformational changes induced by this contact (63). The authors used fluorescence resonance energy transfer to assess the separation of the protein-bound label from the mem-

brane surface (63). The energy transfer data indicated that the distance of closest approach between the protein moiety of placental alkaline phosphatase, used as a model, and the lipid-water interfacial region was smaller than 10–14 Å (63), indicating that the protein portion of the enzyme is very close to the membrane, possibly resting on the surface. Membrane properties can also modulate the catalytic activity of GPI-specific PLC during the cleavage of GPI anchors, and this modulation is also dependent on the characteristics of the phospholipase used (64), with the cleavage efficiency being highly dependent on the lipid composition and properties of the membrane, such as superficial charge and fluidity (62, 65).

NPP1 is plasma membrane-bound, whereas NPP2 is secreted and NPP3 is abundant in intracellular spaces (18). All three NPP isozymes are type II transmembrane glycoproteins characterized by a similar modular structure composed of a short N-terminal intracellular domain, a single transmembrane domain, and a large extracellular domain (66). A putative "EF-hand" Ca^{2+}-binding motif located in the C-terminal part of the extracellular domain is essential for the catalytic activity of NPP1 and NPP3 (66, 67). Active soluble forms of NPP1, NPP2, and NPP3 have been described in serum and conditioned medium (68–73). Human NPP1 transfected in COS7 cells is cleaved close to the transmembrane domain, generating an active soluble enzyme with K^{113}EVKS as the N-terminal sequence (68), and the N-terminal domain of NPP1 and NPP2 is solely responsible as the trafficking pathway of these molecules because an NPP2/NPP1 chimeric construct was secreted and catalytically active (74). We have used this chimeric secreted form of NPP2/NPP1 and fused it to the well characterized GPI-anchoring sequence of human placental alkaline phosphatase (29, 30). This made it possible for us to express, purify, and reconstitute GPI-anchored NPP1 into liposomes using identical conditions as those optimized for TNAP to make proteoliposomes containing TNAP alone, NPP1 alone, or TNAP plus NPP1 together.

Our data show that MV enzymes can be reconstituted into liposomes of predefined composition. Such proteoliposomes proved to be useful in the study of the kinetic interplay of two enzymes present together on biomembrane mimetics when presented with physiological substrates relevant to the biomineralization process. In this paper, we chose to work with PP_i and ATP as the two substrates most likely to be involved in skeletal mineralization. Our data and those of others have conclusively demonstrated that a major role of TNAP is to restrict the size of the extracellular pool of the calcification inhibitor PP_i to allow controlled calcification to proceed (3, 16, 17). The ability of TNAP to use ATP as substrate to initiate calcification has also been documented by many investigators (8, 59, 75, 76), although the details of how ATP-derived P_i participates in calcification remain to be established. Our own work has confirmed that purified TNAP and MVs efficiently hydrolyze ATP as well as its metabolites ADP and AMP (77), in agreement with the broad substrate specificity reported previously for this isozyme (78). We also studied PLP, because abnormal metabolism of this physiological TNAP substrate leads to epileptic seizures and apnea in the most severe forms of hypophosphatasia (27, 79).

Our kinetic analysis revealed that catalysis was mildly to moderately cooperatively regulated by the membrane phospholipids. Furthermore, the simultaneous reconstitution of TNAP and NPP1 into proteoliposomes revealed predominant TNAP activity in PP_i hydrolysis as well as in the sequential degradation of ATP/ADP to ADP/AMP (Figs. 4 and 5). In view of the presence of NPP1 in osteoblasts and MVs, PP_i can theoretically be produced ectoplasmically as well as on the surface of MVs, via hydrolysis of ATP. PP_i, in turn, can be degraded by TNAP, also ectoplasmically and on MVs. Its product, P_i, inhibits TNAP activity (55, 56, 79, 80). The critical balance between these reactions (Fig. 6) is believed to establish a proper steady state P_i/PP_i ratio, conductive to biomineralization. As predicted by Fig. 6, we presently found TNAP to compete with NPP1 for available ATP. However, our kinetic findings suggest that, in MVs, NPP1 may play a smaller role than anticipated from its predominant function on the cytoplasmic membrane of osteoblasts, where it produces PP_i. Comparison of the kinetic behavior of MVs and TNAP-, NPP1-, TNAP + NPP1-containing proteoliposomes revealed that at physiological pH, despite competition between both enzymes for ATP, negligible AMP was produced and that ATP was largely hydrolyzed by TNAP to ADP and further to AMP and to adenosine with high efficiency. Our findings therefore suggest that PP_i is primarily generated ectoplasmically, but around MVs, it is mainly hydrolyzed by TNAP, favoring biomineralization. Thus, TNAP appears to serve two interdependent catalytic roles on the surface of MVs, as a pyrophosphatase and as an ATPase, acting as the single most important enzyme controlling the P_i/PP_i ratio in that vesicular compartment, in agreement with recent data obtained using murine primary osteoblast-derived MVs (77).

The reconstitution of TNAP and NPP1 into proteoliposome membranes allowed us to study the kinetic behavior of two enzymes, critical for biomineralization, present together in a phospholipid microenvironment that adequately recapitulates the native MV microenvironment, in order to evaluate their synergistic and/or antagonistic activity for relevant physiological substrates. This MV biomimetic proteoliposome system can be useful in at least two important translational applications: first, in elucidating the enzymatic defects associated with disease-causing mutations in the TNAP molecule, such as those found in hypophosphatasia (27), which can now be studied in a membrane compartment that better mimic their *in vivo* biological milieu; second, given that this artificial vesicular system adequately mimics the kinetic behavior of the enzymes in the natural vesicular MV environment, this proteoliposome system can be used to screen for small molecule compounds able to modulate (inhibit or activate) TNAP and/or NPP1 activity for potential therapeutic uses (3, 81). Such an approach seems indicated, especially when these compounds bear organic moieties, capable of interacting with membrane phospholipids, directly or indirectly via divalent Ca^{2+}, present in the mineralizing microenvironment. A liposome environment will mimic the phospholipid-modified availability of organic substrates, inhibitors, and modulators to membrane-bound enzymes (*i.e.* allow the study of enzyme catalysis in a more correct manner than with solubilized enzymes). We also expect that this nascent *in vitro* experimental system will allow the reconstruction of pro-

gressively more complex proteoliposomes containing PHOSPHO1 (82), Pit-1/2, ANK, annexins, etc. (83, 84), with the ultimate goal of replicating *in vitro* the events leading to the initiation of HA crystal formation in chondrocyte- and osteoblast-derived MVs.

REFERENCES

1. Boskey, A. (2006) in *Dynamics of Bone and Cartilage Metabolism* (Seibel, M. J., Robins, S. P., and Biezikian, J. P., eds) pp. 201–212, Academic Press, Inc., New York
2. Johnson, K. A., Hessle, L., Vaingankar, S., Wennberg, C., Mauro, S., Narisawa, S., Goding, J. W., Sano, K., Millan, J. L., and Terkeltaub, R. (2000) *Am. J. Physiol. Regul. Integr. Comp. Physiol.* **279,** R1365–R1377
3. Hessle, L., Johnson, K. A., Anderson, H. C., Narisawa, S., Sali, A., Goding, J. W., Terkeltaub, R., and Millan, J. L. (2002) *Proc. Natl. Acad. Sci. U.S.A.* **99,** 9445–9449
4. Ali, S. Y., Sajdera, S. W., and Anderson, H. C. (1970) *Proc. Natl. Acad. Sci. U.S.A.* **67,** 1513–1520
5. Bernard, G. W. (1978) *Clin. Orthop.* **135,** 218–225
6. Morris, D. C., Masuhara, K., Takaoka, K., Ono, K., and Anderson, H. C. (1992) *Bone Miner.* **19,** 287–298
7. Robison, R. (1923) *Biochem. J.* **17,** 286–293
8. Majeska, R. J., and Wuthier, R. E. (1975) *Biochim. Biophys. Acta* **391,** 51–60
9. Fallon, M. D., Whyte, M. P., and Teitelbaum, S. L. (1980) *Lab. Invest.* **43,** 489–494
10. Meyer, J. L. (1984) *Arch. Biochem. Biophys.* **231,** 1–8
11. Moss, D. W., Eaton, R. H., Smith, J. K., and Whitby, L. G. (1967) *Biochem. J.* **102,** 53–57
12. Rezende, A. A., Pizauro, J. M., Ciancaglini, P., and Leone, F. A. (1994) *Biochem. J.* **301,** 517–522
13. Anderson, H. C., Hsu, H. H., Morris, D. C., Fedde, K. N., and Whyte, M. P. (1997) *Am. J. Pathol.* **151,** 1555–1561
14. Anderson, H. C., Sipe, J. B., Hessle, L., Dhamyamraju, R., Atti, E., Camacho, N. P., and Millán, J. L. (2004) Am. *J. Pathol.* **164,** 841–847
15. Anderson, H. C., Harmey, D., Camacho, N. P., Garimella, R., Sipe, J. B., Tague, S., Bi, X., Johnson, K., Terkeltaub, R., and Millán, J. L. (2005) *Am. J. Pathol.* **166,** 1711–1720
16. Harmey, D., Hessle, L., Narisawa, S., Johnson, K. A., Terkeltaub, R., and Millán, J. L. (2004) *Am. J. Pathol.* **164,** 1199–1209
17. Murshed, M., Harmey, D., Millán, J. L., McKee, M. D., and Karsenty, G. (2005) *Genes Dev.* **19,** 1093–1104
18. Terkeltaub, R. A. (2001) *Am. J. Physiol. Cell Physiol.* **281,** C1–C11
19. Huang, R., Rosenbach, M., Vaughn, R., Provvedini, D., Rebbe, N., Hickman, S., Goding, J., and Terkeltaub, R. (1994) *J. Clin. Invest.* **94,** 560–567
20. Johnson, K., Moffa, A., Chen, Y., Pritzker, K., Goding, J., and Terkeltaub, R. (1999) *J. Bone Miner. Res.* **14,** 883–892
21. Hashimoto, S., Ochs, R. L., Rosen, F., Quach, J., McCabe, G., Solan, J., Seegmiller, J. E., Terkeltaub, R., and Lotz, M. (1998) *Proc. Natl. Acad. Sci. U.S.A.* **95,** 3094–3099
22. Terkeltaub, R., Rosenbach, M., Fong, F., and Goding, J. (1994) *Arthritis Reum.* **37,** 934–941
23. Ciancaglini, P., Simão, A. M., Camolezi, F. L., Millán, J. L., and Pizauro, J. M. (2006) *Br. J. Med. Biol. Res.* **39,** 603–610
24. Camolezi, F. L., Daghastanli, K. P. R., Magalhães, P. P., Pizauro, J. M., and Ciancaglini, P. (2002) *Int. J. Biochem. Cell Biol.* **1282,** 1–11
25. Ierardi, D. F., Pizauro, J. M., and Ciancaglini, P. (2002) *Biochim. Biophys. Acta* **1567,** 183–192
26. Murphy, W., and Messersmith, P. B. (2000) *Polyhedron* **19,** 357–363
27. Di Mauro, S., Manes, T., Hessle, L., Kozlenkov, A., Pizauro, J. M., Hoylaerts, M. F., and Millán, J. L. (2002) *J. Bone Miner. Res.* **17,** 1383–1391
28. Gijsbers, R., Ceulemans, H., and Bollen, M. (2003) *Biochem. J.* **371,** 321–330
29. Millán, J. L. (1986) *J. Biol. Chem.* **261,** 3112–3115
30. Micanovic, R., Bailey, C. A., Brink, L., Gerber, L., Pan, Y. C., Hulmes, J. D., and Udenfriend, S. (1988) *Proc. Natl. Acad. Sci. U.S.A.* **85,** 1398–1402
31. Simão, A. M., Beloti, M. M., Cezarino, R. M., Rosa, A. L., Pizauro, J. M., and Ciancaglini, P. (2007) *Comp. Biochem. Physiol. A Mol. Integr. Physiol.* **146,** 679–687
32. Ciancaglini, P., Pizauro, J. M., Rezende, A. A., Rezende, L. A., and Leone, F. A. (1990) *Int. J. Biochem.* **22,** 385–392
33. Hartree, E. F. (1972) *Anal. Biochem.* **48,** 422–427
34. Pizauro, J. M., Ciancaglini, P., and Leone, F. A. (1995) *Mol. Cell Biochem.* **152,** 121–129
35. Leone, F. A., Baranauskas, J. A., Furriel, R. P., Borin, I. A., and Sigraf, W. (2005) *Biochem. Mol. Educ.* **33,** 399–403
36. New, R. R. C. (1990) *Liposomes: A Practical Approach*, Oxford University Press, New York
37. Prasad, R. (1996) *Manual of Membrane Lipids* (Prasad, R., ed) Springer-Verlag, Berlin
38. Kirsch, T., Nah, H. D., Shapiro, I. M., and Pacifici, M. (1997) *J. Cell Biol.* **137,** 1149–1160
39. Wu, L. N., Genge, B. R., Dunkelberger, D. G., LeGeros, R. Z., Concannon, B., and Wuthier, R. E. (1997) *J. Biol. Chem.* **272,** 4404–4411
40. Wu, L. N., Genge, B. R., Kang, M. W., Arsenault, A. L., and Wuthier, R. E. (2002) *J. Biol. Chem.* **277,** 5126–5133
41. Damek-Poprawa, M., Golub, E., Otis, L., Harrison, G., Phillips, C., and Boesze-Battaglia, K. (2006) *Biochemistry* **45,** 3325–3336
42. Kunitake, T., Okahata, Y., Tamaki, K., Kumamaru, F., and Takayanagi, M. (1977) *Chem. Lett.* 387–390
43. Benatti, C. R., Feitosa, E., Fernandez, R. M., and Lamy-Freund, M. T. (2001) *Chem. Phys. Lipids* **111,** 93–104
44. Benatti, C. R., Epand, R. M., and Lamy, M. T. (2007) *Chem. Phys. Lipids* **145,** 27–36
45. Arien, A., and Dupuy, B. (1997) *J. Microencapsul.* **14,** 753–760
46. Kirsch, T., Wang, W., and Pfander, D. (2003) *J Bone Miner. Res.* **18,** 1872–1881
47. Sela, J., Gross, U. M., Kohavi, D., Shani, J., Dean, D. D., Boyan, B. D., and Schwartz, Z. (2000) *Crit. Rev. Oral Biol. Med.* **11,** 423–436
48. Liu, C., Marshall, P., Schreibman, I., Vu, A., Gai, W., and Whitlow, M. (1999) *Blood* **93,** 2297–2301
49. Bellet-Amalric, E., Blaudez, D., Desbat, B., Graner, F., Gauthier, F., and Renault, A. (2000) *Biochim. Biophys. Acta* **1467,** 131–143
50. Ronzon, F., Desbat, B., Chauvet, J. P., and Roux, B. (2002) *Biochim. Biophys. Acta* **1560,** 1–13
51. Eanes, E. D., and Hailer, A. W. (1985) *Calcif. Tissue Int.* **37,** 390–394
52. Eanes, E. D. (1989) *Anat. Rec.* **224,** 220–225
53. Storch, J., and Kleinkeld, A. M. (1985) *Trends Biochem. Sci.* **10,** 418–421
54. Carruthers, A., and Melchior, D. L. (1986) *Trends Biochem. Sci.* **11,** 331–335
55. Pizauro, J. M., Curti, C., Ciancaglini, P., and Leone, F. A. (1987) *Comp. Biochem. Physiol.* **87B,** 921–926
56. Rezende, L. A., Ciancaglini, P., Pizauro, J. M., and Leone, F. A. (1998) *Cell Mol. Biol.* **44,** 293–302
57. Leone, F. A., Rezende, L. A., Ciancaglini, P., and Pizauro, J. M. (1998) *Int. J. Biochem. Cell Biol.* **30,** 89–97
58. Curti, C., Pizauro, J. M., Rossinholi, G., Vugman, I., Mello de Oliveira, J. A., and Leone, F. A. (1986) *Cell Mol. Biol.* **32,** 55–62
59. Demenis, M. A., and Leone, F. A. (2000) *IUBMB Life* **49,** 113–119
60. Sesana, S., Re, F., Bulbarelli, A., Salerno, D., Cazzaniga, E., and Masserini, M. (2008) *Biochemistry* **47,** 5433–5440
61. Hoylaerts, M. F., Manes, T., and Millán, J. L. (1997) *J. Biol. Chem.* **272,** 22781–22787
62. Lehto, M. T., and Sharom, F. J. (1998) *Biochem. J.* **332,** 101–109
63. Lehto, M. T., and Sharom, F. J. (2002) *Biochemistry* **41,** 8368–8376
64. Sharom, F. J., McNeil, G. L., Glover, J. R., and Seier, S. (1996) *Biochem. Cell Biol.* **74,** 701–713
65. Lehto, M. T., and Sharom, F. J. (2002) *Biochemistry* **41,** 1398–1408
66. Bollen, M., Gijsbers, R., Ceulemans, H., Stalmans, W., and Stefan, C. (2000) *Crit. Rev. Biochem. Mol. Biol.* **35,** 393–432
67. Andoh, K., Piao, J. H., Terashima, K., Nakamura, H., and Sano, K. (1999) *Biochim. Biophys. Acta* **1446,** 213–224
68. Hosoda, N., Hoshino, S. I., Kanda, Y., and Katada, T. (1999) *Eur. J. Biochem.* **265,** 763–770

69. Belli, S. I., van Driel, I. R., and Goding, J. W. (1993) *Eur. J. Biochem.* **217,** 421–428
70. Stracke, M. L., Krutzsch, H. C., Unsworth, E. J., Arestad, A., Cioce, V., Schiffmann, E., and Liotta, L. A. (1992) *J. Biol. Chem.* **267,** 2524–2529
71. Murata, J., Lee, H. Y., Clair, T., Krutzsch, H. C., Arestad, A. A., Sobel, M. E., Liotta, L. A., and Stracke, M. L. (1994) *J. Biol. Chem.* **269,** 30479–30484
72. Meerson, N. R., Delautier, D., Durand-Schneider, A. M., Moreau, A., Schilsky, M. L., Sternlieb, I., Feldmann, G., and Maurice, M. (1998) *Hepatology* **27,** 563–568
73. Frittitta, L., Camastra, S., Baratta, R., Costanzo, B. V., D'Adamo, M., Graci, S., Spampinato, D., Maddux, B. A., Vigneri, R., Ferrannini, E., and Trischitta, V. (1999) *J. Clin. Endocrinol. Metab.* **84,** 3620–3625
74. Jansen, S., Stefan, C., Creemers, J. W., Waelkens, E., Van Eynde, A, Stalmans, W., and Bollen, M. (2005) *J. Cell Sci.* **118,** 3081–3089
75. Hsu, H. H., and Anderson, H. C. (1996) *J. Biol. Chem.* **271,** 26383–26388
76. Hsu, H. H., Camacho, N. P., and Anderson, H. C. (1999) *Biochim. Biophys. Acta* **1416,** 320–332
77. Ciancaglini, P., Yadav, M. C., Simão, A. M. S., Narisawa, S., Pizauro, J. M., Farquharson, C. D., Hoylaerts, M. F., and Millán, J. L. (2010) *J. Bone Miner. Res.* 10.1359/jbmr.091023
78. Say, J. C., Ciuffi, K., Furriel, R. P., Ciancaglini, P., and Leone, F. A. (1991) *Biochim. Biophys. Acta* **1074,** 256–262
79. Millán, J. L. (2006) *Mammalian Alkaline Phosphatases: From Biology to Applications in Medicine and Biotechnology*, Wiley-VCH Verlag GmbH & Co., pp. 1–322, Weinheim, Germany
80. Leone, F. A., Pizauro, J. M., and Ciancaglini, P. (1997) *Trends Comp. Biochem. Physiol.* **3,** 57–73
81. Sergienko, E., Su, Y., Chan, X., Brown, B., Hurder, A., Narisawa, S., and Millán, J. L. (2009) *J. Biomol. Screen.* **14,** 824–837
82. Roberts, S., Narisawa, S., Harmey, D., Millán, J. L., and Farquharson, C. (2007) *J Bone Miner. Res.* **22,** 617–627
83. Balcerzak, M., Radisson, J., Azzar, G., Farlay, D., Boivin, G., Pikula, S., and Buchet, R. (2007) *Anal. Biochem.* **361,** 176–182
84. Xiao, Z., Camalier, C. E., Nagashima, K., Chan, K. C., Lucas, D. A., de la Cruz, M. J., Gignac, M., Lockett, S., Issaq, H. J., Veenstra, T. D., Conrads, T. P., and Beck, G. R., Jr. (2007) *J. Cell Physiol.* **210,** 325–335